# A Study of the Effect of Nanoscale VC Precipitate on the Mechanical Properties of Microalloyed Steel using the Finite Element Method

Wu Zhaoyu[1,2]
[1] Panxi Science and Technology Innovation Center, Panzhihua University
Panzhihua, 617000, China.
[2] *Department of Equipment Manufacturing*, Chengdu Industrial Vocational Technical College
Chengdu, 610218, China
wuzhaoyu@shu.edu.cn

***Abstract* — In this paper we use finite element computations to study the effect of nanoscale size of Vanadium Carbide (VC) precipitate on the mechanical properties of high strength low alloy steels. By comparing the models of real structure with finite element model, we found that the strength increases with the decrease of the precipitate sizes, while the change of ductility is increased. Our results also showed that the elastic and plastic anisotropy are induced by VC precipitates generated in the tensile deformation process. There is high equivalent stress and no plastic deformation in VC precipitates. Furthermore, we investigated the interaction of dislocation and VC precipitates by analyzing the stress distribution in VC precipitates, which indicated that when the precipitates size is10 nm it can more effectively improve the mechanical properties of the microalloyed steels.**

***Keywords - component; nanoscale VC precipitates; finite element method; dislocation; mechanical properties***

## I. INTRODUCTION

High strength low alloy (HSLA) steels, which contain small amount of alloying elements such as Nb, V, or Ti, etc, have been widely used in the pipeline and automotive sector applications [1]. The micro alloying elements facilitate grain refinement through carbonitride precipitation in the austenite and contribute to dispersion hardening through carbide precipitation in supersaturated ferrite during or after the austenite-ferrite transformation[2]. These steels exhibit an outstanding combination of high tensile strength, good toughness, resistance to brittle fracture and good weld ability[3]. The HSLA steels derivehighstrength from a combination of mechanisms including solid solution strengthening, grain size refinement, dislocation strengthening and precipitation hardening[4]. Fine MX carbide precipitates and carbonitride precipitates interact with dislocations at the grain boundaries and subgrainboundaries during thermo-mechanical processing of micro-alloyed steels [5-8]. These carbide precipitates play a significant role in dislocation motion which can be inhibited because of the pining (precipitate-dislocation interaction) and precipitation hardening effect [9-11]. The fine size of precipitates is among 1-100nm, or the mechanical properties of material will be decreased due to the coarse precipitates [12-14].The mechanical properties of steels can be influenced by several factors, such as crystallography and dimensions, volume fractions, distributions of nanoscale precipitates [15,16]. Additionally, all types of soft precipitation and hard precipitation have significant influence on mechanical properties of micro alloyed steel. In particularly, the hard precipitation of VC, TiC, NbC plays an important role in micro alloyed steel.

Though the influence of vanadium on grain refinement is less than that of niobium, it does have similar role with niobium on the grain refinement. Nb, V has advantages as a microalloying element due to its greater solubility in austenite. However, it may provide a greater degree of precipitation hardening at lower temperatures [17]. Meanwhile, it has also been reported that addition of V benefits the impact toughness and corrosion properties of steels, which is associated with the removal of coarse Cr carbonitrides from the grain boundary[18]. It is observed that the precipitates distributed as either dispersed precipitation or interphase precipitation, in ferrite regions and dislocations [19,20]. The excellent strength and elongation of HSLA steel are attributed to nanoscale precipitates and microstructure of material. The other strengthening factors of these precipitates are analyzed by taking into account of the interaction with dislocation strengthening [21-23].

In this work, Finite Element Method (FEM) is employed to analyze the effect of different size of VC precipitates on mechanical properties in uniaxial tensile deformation. To explore the strengthening mechanism of VC precipitates different microstructure models were based on real micrographs containing VC precipitates which are randomly dispersed in the matrix.

## II. FINITE ELEMENT MODEL

### *A. FEM and Material Description*

In the previous work [15], the atomic structure and microstructure of carbide in high-strength low-alloy (HSLA) steel which was tempering at 650°C for 4h were

characterized using atom probe tomography (APT) and transmission electron microscopy (TEM). In order to investigate the effect of VC precipitation on the mechanical properties of microalloyed steel, a finite element model has been established containing nanoscale VC precipitates and matrix of microstructure according to the microstructure observed by previous experiment (Fig.1).In this work, a Mat lab script has been developed to establish two full microscopic Voronoi grains of 2D micromechanical finite element modelsandmanually fit random circles for VC precipitations. In the simulation, perfect bonding between the matrix and the precipitated precipitates is assumed. It is important to point out that the VC precipitates are randomly distributed with arbitrary shapes in reality, but they are considered circular shapes in this work as shown in Fig.1(c). The parameters of VC precipitates and matrix are summarized in Table 1. The quantity E denotes the Young's modulus, ν denotes the Poisson ratio, G is the shear modulus, b is the Burger's vector, and C is a constant. The flow response highly depends on the development of the internal changes in the material's microstructure. The total strain rate is assumed to be separable into internal and precipitate strains. The constitutive model used in this work is same to our previous work [16].

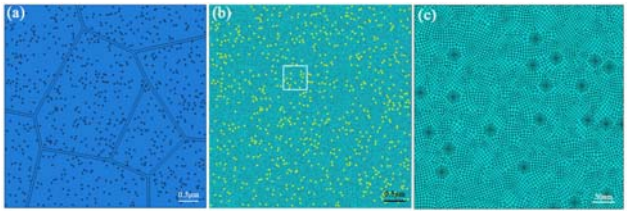


Fig.1. Finite element model of VC precipitates: (a) no meshing model, (b) meshing model, (c) enlarged view

TABLE 1. SIMULATION PARAMETERS OF VC PRECIPITATES AND MATRIX

| | E (GPa) | ν | G (GPa) | C | b ($10^{-9}$m) |
|---|---|---|---|---|---|
| **VC Precipitates** | 430 | 0.189 | 180.8 | 0.3 | 0.43 |
| **Matrix** | 210 | 0.3 | 80.8 | 0.3 | 0.29 |

### *B. Simulation Process*

To research the effect of VC precipitates size on mechanical properties of micro-alloyed steels, finite element (FE) software, ABAQUS, is used to establish composite model which contains nanoscale VC precipitation and matrix. VC precipitates with different sizes are randomly distributed in matrix. In the model, the VC precipitates are modeled as circular areas with radius of 10, 15 and 20 nm, respectively. It is important to mention that the multi-cell finite element model shown in Fig.1(a) is asymmetric. The numerical model is constructed using two-dimensional four-node plane stress and strain elements model (CPE4 and CPS4 in ABAQUS). The adequacy of the finite element discretization is checked by repeating a calculation using refined meshes until a satisfactory computational accuracy is obtained. The boundary condition of the finite element model is shown in Fig.2 with square dimension of a side length of 5μm. Displacement boundary conditions of FEM plane uniaxial tension is performed for every specimen. And movement in the vertical direction of uniaxial tension on the left edge is free and a monotonic tensile displacement of 0.3μm (U = 0.3μm) in horizontal direction is applied on the right edge as shown in Fig.2.

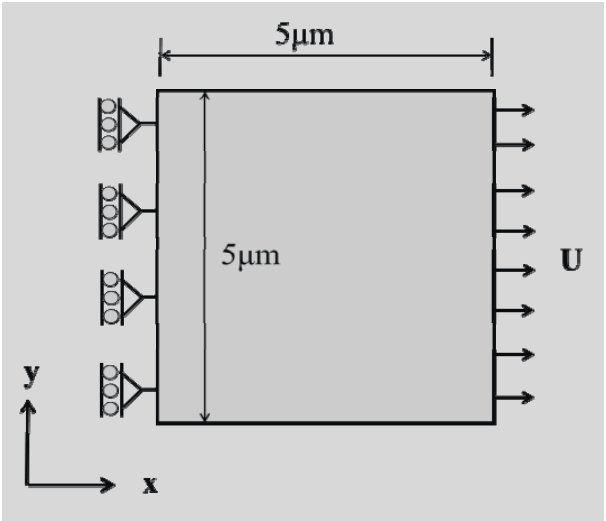


Fig.2. Example of boundary conditions and loads.

## III. RESULTS AND DISCUSSION

### *A. Effect on the Strain Component LE11 in Different Sizes of VC Precipitates*

For two-phase composites, volume fractions of VC precipitates is 1 % (φ = 1 %) and the applied strain of composites model is 6%. The diameters of VC precipitates are 10 and 20 nm, respectively, with corresponding typical element number of 653837 and 348275 in the FE models. The precipitates correlation and stress–strain characteristics of microalloyed steel is analyzed as displayed in Fig.3. The correlation between size of precipitates and stress–strain characteristics of microalloyed steel is analyzed as displayed in Fig.3, which shows the contours of the equivalent stress and the strain component LE11 along the loading direction in different sizes of VC precipitates. The simulation results show that the largest equivalent stress takes place at the center of VC precipitates. In addition, the largest strain component LE11 of matrix material occurs around VC precipitates. It can be seen that the equivalent stress and the strain component LE11 display a "butterfly-shaped" distribution. From the simulation results, it can be confirmed that the largest equivalent stress decreases but the largest strain component LE11 increases first and then declines with the increasing size of VC precipitates. The largest equivalent stress is about 1481MPa, 1297 MPa when the VC precipitates size is10, 20 nm, respectively. It is clear that the

more VC precipitates smaller, the more equivalent stress higher. It is reasonable to believe that the simulation results are attributed to high dislocation density around smaller size of VC precipitates[24],therefore a higher stress is acquired surrounding smaller sizes of VC precipitates. Additionally, there is a critical particle size where the strengthening nanoscale VC precipitates is the largest.

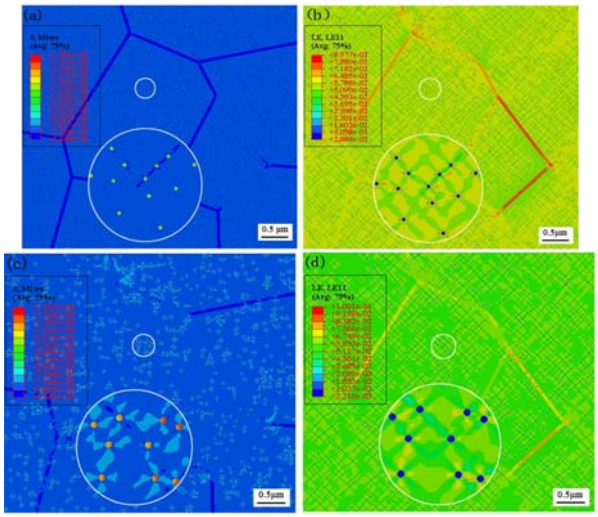


Fig.3 Contours of the equivalent stress and the strain component LE11 of VC precipitates: (a) (b) 10nm; (c) (d) 20nm

The contours of equivalent stress in matrix material are calculated in Fig.4 (a) and (c), with different sizes of VC precipitates, equivalent stress contours were little change. Also, higher equivalent stress exist surrounding VC precipitates and displays a "butterfly-shaped" distribution, where equivalent stress in horizontal and loading directions is bigger.

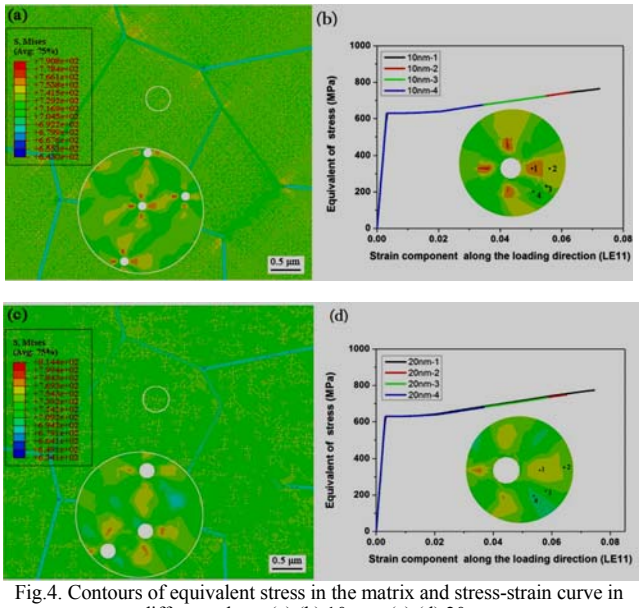


Fig.4. Contours of equivalent stress in the matrix and stress-strain curve in different place: (a) (b) 10 nm; (c) (d) 20 nm

However, contours are also observed that the development of lower equivalent stress at oriented 45° angle with the loading axis in the composite matrix. According to shear slip mechanisms of dislocation movement [25-27], the slip system is more easily activated along 45° orientation. Therefore, it is evident that there exist lower equivalent stress along 45° orientation with the tensile direction. It is obviously found that the equivalent stress exist in matrix differently along different directions. Thus this phenomenon well explains the fact that the anisotropic property exists in matrix around VC precipitates. The effect of precipitate size on the matrix at different location, and the relationship of stress–strain are analyzed as shown in Fig.4（b）and（d）. The results indicate that the equivalent stress and the strain component LE11 descend in order at location of point 1,2,3,4. Therefore, the response of stress and strain of material decline sequentially at those positions.

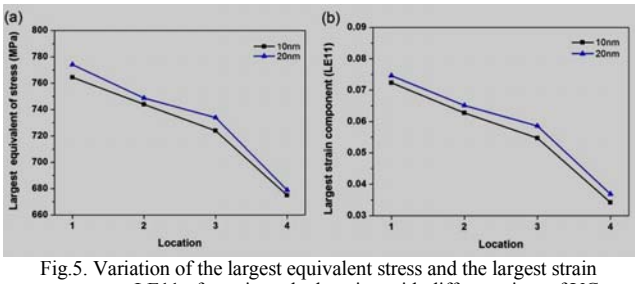


Fig.5. Variation of the largest equivalent stress and the largest strain component LE11 of matrix at the location with different sizes of VC precipitates

In addition, Fig.5 (a) – (b) also shows that both the equivalent stress and the strain component LE11 change nonlinearly at different place. However, with the size of VC precipitates increasing, the largest equivalent stress and the strain component LE11 was declined. Furthermore, it can be observed that the simulation results are in good agreement with the precipitation strengthening theory, which is possible to estimate the dislocation strengthening resulting from the VC precipitates as obstacles to dislocations[24,28].It also can be found that the matrix is effectively strengthened by VC precipitates with the size of 15 nm about the nonlinear stress-strain response in matrix from the Fig.5.

The equivalent stress and the strain component LE11 distribute in matrix without VC precipitates according to certain reference value of stress was shown in Fig.6. Contours indicate that the response of stress region is consistent with strain. The strain component LE11was higher as the equivalent stress take place at the same regions. As shown in Fig.6 (c) and (d), the larger stress and strain occur in matrix around 20 nm VC precipitates.

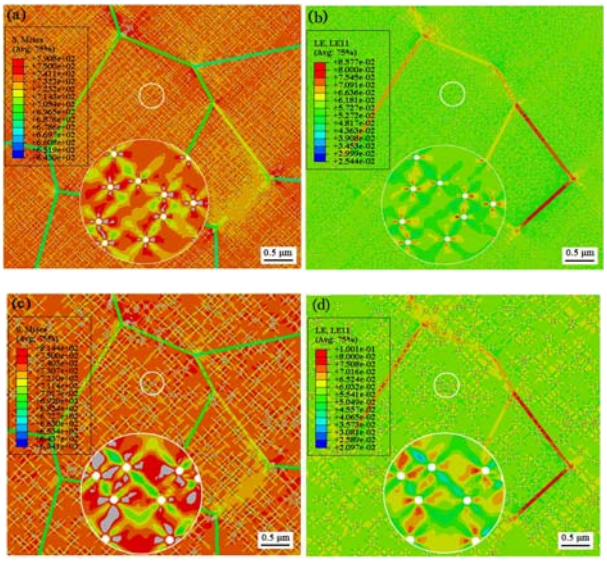


Fig.6. Contours of VC precipitates of equivalent stress and strain component LE11 in matrix: (a) (b) 10 nm; (c) (d) 20 nm

### *B. The Evolution of Mechanical Properties and Interaction Between Precipitates and Dislocations in Low Carbon Micro-Alloyed Steels*

FEM calculation indicates that the equivalent stress is higher than 1100MPa in VC precipitates for all three sizes.Fig.7 shows the contour plots of equivalent stress and strain component LE11 in different sizes of VC precipitates. Additionally, the strain component LE11 is in a very low value of about 0.3% and the equivalent plastic strain is zero in VC precipitates, this result shows that the VC precipitates only exists elastic deformation without plastic deformation. It is well known that the VC precipitate possesses a relatively high Vickers hardness (33.3 ± 0.5 GPa) and Young's modulus (436 ± 8 GPa) [29], which is similar to ceramics. Therefore, the VC precipitates exhibit high strength during deformation process. In addition, there is high dislocation density around VC precipitates. Therefore, the considerable dominance of fine-scale precipitation on dislocations is an important strengthening mechanism in the investigated steels. Fig.7 (a) – (f) shows the contour plots of equivalent stress and strain component LE11 in different sizes of VC precipitations. From the contours in Fig.7 (a) and (d), it can be found that the larger equivalent stress and strain component LE11 takes place at the right of VC precipitates when the VC precipitates size of 10 nm and 20 nm. However, the contour plots of stress and strain have significant difference between 10 nm and 20 nm of VC precipitates. The largest equivalent stress of 10 nm is higher than that of 20 nm. For 15 nm VC precipitates, the larger equivalent stress and strain component LE11 takes place at the center of VC precipitates, thus leads to a higher flow stress in matrix with higher strengthening as shown in Fig.7. Essentially, precipitation strengthening is achieved by producing a particulate dispersion of obstacles to dislocation movement, which the precipitates dispersion being achieved by a second phase precipitation process and the nature of the interaction of the precipitates with dislocations[30]. A variety of mechanisms has been proposed, involving precipitate bypassing by Orowan looping and precipitate shearing. In the case of hardness, the small size of VC precipitate is soft while the large size of VC precipitates is hard. Accordingly, the soft VC precipitates strengthening increases with increasing of precipitate size, whereas the hard VC precipitate strengthening decreases with increased precipitate spacing (increasing VC precipitate size).For larger precipitates, the upper limit of this form of strengthening is imposed by the transition to the classical Orowan looping process. The strength of the dislocation-VC precipitate repulsion force in connection with 'soft' precipitate strengthening is important in dictating the critical precipitate size at which the transition to 'hard' precipitate strengthening occurs and, therefore, the magnitude of the strengthening contribution at this transitional precipitate size. From above discussed, the VC precipitate of 20 nm is more available to strengthen material as shown in Fig.7.

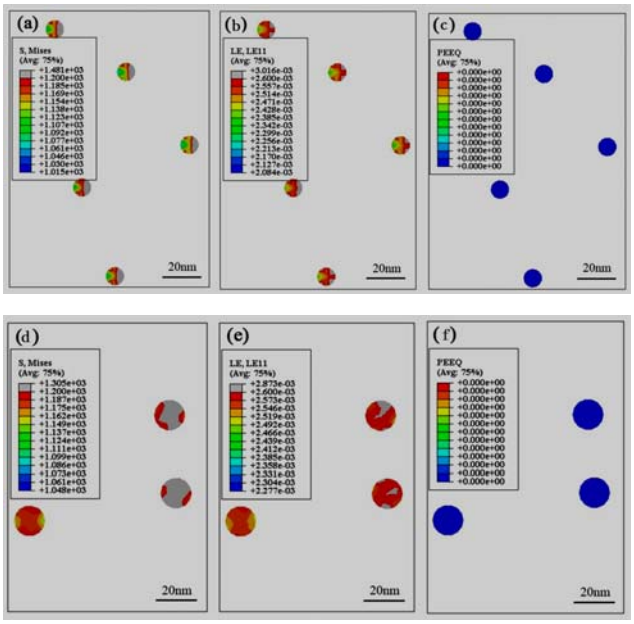


Fig.7. The Contours of Equivalent Stress, The Strain Component LE11 and The Equivalent Plastic of Strain in Difference Size of VC Precipitates: (a), (b), (c), 10mm; (d), (e), (f) 20mm.

The template is used to format your paper and style the text. All margins, column widths, line spaces, and text fonts are prescribed; please do not alter them. You may note peculiarities. For example, the head margin in this template measures proportionately more than is customary. This measurement and others are deliberate, using specifications that anticipate your paper as one part of the entire proceedings, and not as an independent document. Please do not revise any of the current designations.

### *C. The Equivalent Stress-Strain Component LE11 Curves of the Matrix Embodied with VC Precipitates with Different Size*

In previous work, the effect of size of Cu (soft particle) precipitation on the mechanical properties of microalloyed steel is investigated, and it not found "folded back" regions at the center of Cu precipitates16. The stress-strain of "folded back" regions are analogous in different sizes of VC precipitates, both the start point (A) and end point (C) of curves have no significant difference. It is evident that the "folded back" stage not sensitive to the size of VC precipitates as shown in Table.2.

TABLE 2. THE EQUIVALENT STRESS AND STRAIN COMPONENT LE11 IN THE"FOLDED BACK"OF A AND B POINT IN DIFFERENT SIZE VC PRECIPITATES

| VC Precipitates (nm) | LE11 at Point A ($10^{-3}$) | S,mises at Point A (Mpa) | LE11 at Point B ($10^{-3}$) | S,Mises at Point B (Mpa) |
|---|---|---|---|---|
| 10 | 1.8448 | 812.15 | 1.7928 | 783.39 |
| 20 | 1.8417 | 810.26 | 1.7850 | 779.05 |

In order to analyze the cause of "folded back" region, we present the change of stress in VC precipitates with different size in Fig.8, which are the equivalent stress contour corresponding to "folded back" region. For VC precipitates of 10nm, the contours of equivalent stress distribution are shown in Fig.8. It can be observed that the higher equivalent stress almost all occur at the left of VC precipitates (Fig.8). At the the beginning of descending stage, it is clearly suggested that the interaction between the dislocations and VC precipitates has become stronger at this stage. At the same time, original plastic deformation is generated in the matrix with the tensile deformation.

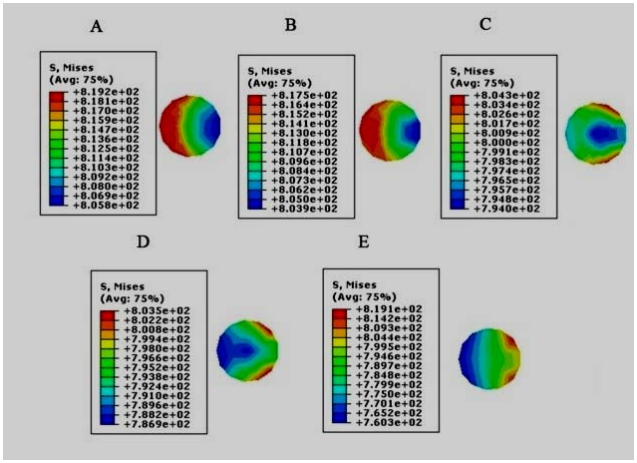


Fig.8.The contours of equivalent stress in "folded back" (A to B) region for different sizes of VC precipitates 10nm

If the precipitate size is smaller, the precipitate is relatively 'softer', it is sheared by the dislocation quickly with the deformation, as shown in Fig.9. After the VC precipitates being sheared by the dislocations, the dislocations produce a tack stacking fault at the right of VC precipitates. Therefore, it is observed that the higher equivalent stress occur at the right of VC precipitates Fig.9. It can well explain the simulation results above all. Additionally, it previous suggested that the small size of nanoscale VC precipitates have size effect. So that the HSLA materials can be strengthen by nanoscale precipitates.

The strengthening mechanism of dislocation movement which is the schematic diagram of precipitates being sheared and the dislocation passing through precipitates is shown in Fig.12 (d).

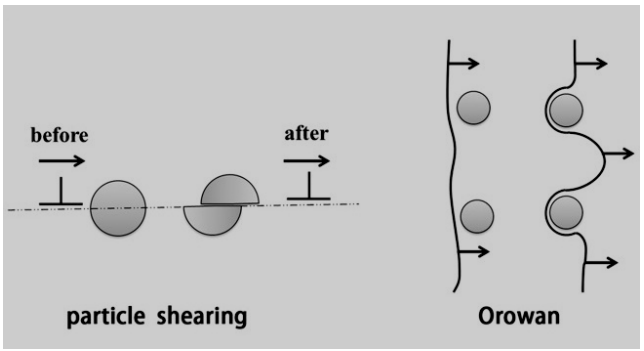


Fig.9. The contours of equivalent stress in "folded back" (A to B) region for different sizes of VC precipitates: (a) 10nm; (b) 15nm; (c) 20nm; (d) dislocation movement mechanism

## IV. Conclusions

Finite element model was successfully applied to study the effects of nanoscale VC precipitates on the deformation behavior of HSLA. The simulation captured the VC precipitates and matrix characteristics in detail, such as strengthening pattern, critical size of VC precipitates strengthening, anisotropic properties and interaction between dislocation and VC precipitates. The main observations can be summarized as follows:

(1) It has been demonstrated that the response of stress and strain of surrounding VC precipitates are larger than that in the matrix during uniaxial tensile deformation. The contours of equivalent stress and strain component LE11 display anisotropy in the matrix.

(2) The high equivalent stress occurs at VC precipitates but that there is on plastic deformation. Due to the interaction between the dislocation and precipitates, there is "folded back" phenomenon on stress-strain curve of VC precipitates, which explains the Ashby-Orowan relationship between dislocation and VC precipitates.

(3) The effect of VC precipitate size is the main factor improving the strength of the matrix. The numerical analysis of flow stress of HSLA during tensile deformation shows that the strength of whole material decreases.

(4) The elongation increase when the size of VC precipitates increases. The results show that VC precipitate with size of 10-15 nm is more available to strengthen the material compared with the material without VC precipitates.

## ACKNOWLEDGMENT

The authors would like to thank Qiaofen Zhang for the support during simulation calculation. This work was supported by the Science and technology plan projects of Panzhihua. [No.2015CY-G-23].

## REFERENCES

[1] B.K. Show, R. Veerababu, R. Balamuralikrishnan & G. Malakondaiah. Effect of vanadium and titanium modification on the microstructure and mechanical properties of a microalloyed HSLA steel. Mater. Sci. Eng.A. 527, (2010) 1595-1604.

[2] T.P. Wang, F.H. Kao, S.H. Wang, J.R. Yang, C.Y. Huang & H.R. Chen. Isothermal treatment influence on nanometer-size carbide precipitation of titanium-bearing low carbon steel. Mater. Lett. 65, (2011) 396-399.

[3] P.C.M. Rodrigues, E.V. Pereloma & D.B. Santos. Mechanical properities of an HSLA bainitic steel subjected to controlled rolling with accelerated cooling. Mater. Sci. Eng. A. 283, (2000) 136-143.

[4] J. Chen, M. Lv, S. Tang, Z. Liu & G. Wang. Influence of cooling paths on microstructural characteristics and precipitation behaviors in a low carbon V–Ti microalloyed steel. Mater. Sci. Eng.A. 594, (2014) 389-393.

[5] F.Z. Bu, X.M. Wang, L. Chen, S.W. Yang, C.J. Shang & R.D.K. Misra. Influence of cooling rate on the precipitation behavior in Ti–Nb–Mo microalloyed steels during continuous cooling and relationship to strength. Mater. Charact. 102, (2015) 146-155.

[6] Z.W. Peng, L.J. Li, J.X. Gao & X.D. Huo. Precipitation strengthening of titanium microalloyed high-strength steel plates with isothermal treatment. Mater. Sci. Eng. A. 657, (2016) 413-421.

[7] S.G. Hong, H.J. Jun, K.B. Kang & C.G. Park. Evolution of precipitates in the Nb–Ti–V microalloyed HSLA steels during reheating. Scripta. Mater. 48, (2003) 1201-1206.

[8] S.S. Campos, E.V. Morales & H.J. Kestenbach. Detection of interphase precipitation in microalloyed steels by microhardness measurements. Mater. Charact. 52, (2004) 379-384.

[9] R.D.K. Misra, H. Nathani, J.E. Hartmann & F. Siciliano. Microstructural evolution in a new 770MPa hot rolled Nb–Ti microalloyed steel. Mater. Sci. Eng. A. 394, (2005) 339-352.

[10] Z. Jia, R.D.K. Misra, R. O'Malley & S.J. Jansto. Fine-scale precipitation and mechanical properties of thin slab processed titanium–niobium bearing high strength steels. Mater. Sci. Eng. A. 528, (2011) 7077-7083.

[11] C.Y. Chen, C.C. Chen & J.R. Yang. Synergistic effect of austenitizing temperature and hot plastic deformation strain on the precipitation behavior in novel HSLA steel. Mater. Sci. Eng. A. 639, (2015) 145-154.

[12] I.B. Timokhina, P.D. Hodgson, S.P. Ringer, R.K. Zheng & E.V. Pereloma. Precipitate characterisation of an advanced high-strength low-alloy (HSLA) steel using atom probe tomography. Scripta Mater. 56, (2007) 601-604.

[13] Q.D. Liu, W.Q. Liu & S.J. Zhao. Solute Behavior in the Initial Nucleation of V- and Nb-Containing Carbide. Metall. Mater. Trans. A. 42, (2011) 3952-3960.

[14] W. Zhou, H. Guo, Z. Xie, X. Wang & C. Shang. High strength low-carbon alloyed steel with good ductility by combining the retained austenite and nano-sized precipitates. Mater. Sci. Eng. A. 587, (2013) 365-371.

[15] Q.D. Liu, W.Q. Liu & S.J. Zhao. Combination of TEM and 3D atom probe study of microstructure and alloy carbide in a Nb-V micro-alloyed steel tempered at 650 °C. Met. Mater. int. 19, (2013) 777-782.

[16] L. Hu, S.J. Zhao & Q. Liu. The effect of size of Cu precipitation on the mechanical properties of microalloyed steel. Mater. Sci. Eng. A. 556, (2012) 140-146.

[17] R. Lagneborg, T. Siwecki, S. Zajac & B. Hutchinson. Role of vanadium in microalloyed steels. Scand. J. Metall. 28, (1999) 186-241.

[18] J. Han, H. Li, F. Barbaro, L. Jiang, Z. Zhu, H. Xu & L. Ma. Precipitation and impact toughness of Nb–V stabilised 18Cr–2Mo ferritic stainless steel during isothermal aging. Mater. Sci. Eng. A. 612, (2014) 63-70.

[19] R. Paton. Notch and Fracture Toughness Studies on Stainless Steels Containing Vanadium. ISIJ. Int. 38, (1998) 1007-1014.

[20] F.A. Khalid. Precipitation and compositional changes in the structural phases of microalloyed automotive steels. Mater. Sci. Eng. A. 325, (2002) 281-285.

[21] M. Charleux, W.J. Poole, M. Militzer & A. Deschamps. Precipitation behavior and its effect on strengthening of an HSLA-Nb/Ti steel. Metall. Mater. Trans. A. 32, (2001) 1635-1647.

[22] X.P. Wang, A.M. Zhao, Z.Z. Zhao, Y. Huang, Z.D. Geng & Y. Yu. Precipitation Strengthening by Nanometer-sized Carbides in Hot-rolled Ferritic Steels. Jion. Steel. Res Int. 21, (2014) 1140-1146.

[23] C.F. Meng, Y.D. Wang, Y.H. Wei, B.Q. Shi, T.X. Cui & Y.T. Wang. Strengthening Mechanisms for Ti- and Nb-Ti-micro-alloyed High-strength Steels. Jion. Steel. Res Int. 23, (2016) 350-356.

[24] M.A. Altuna, A. Iza-Mendia & I. Gutiérrez. Precipitation of Nb in Ferrite After Austenite Conditioning. Part II: Strengthening Contribution in High-Strength Low-Alloy (HSLA) Steels. Metall. Mater. Trans. A. 43, (2012) 4571-4586.

[25] G.I. Taylor. The Mechanism of Plastic Deformation of Crystals. Part I. Theoretical. Proceedings of the Royal Society of London. Series A, Containing Papers of a Mathematical and Physical Character 145, (1934) 362-387.

[26] G. Winther & X. Huang. Dislocation structures. Part II. Slip system dependence. Philos. Mag. 87, (2007) 5215-5235.

[27] K. Inal, P.D. Wu & K.W. Neale. Instability and localized deformation in polycrystalline solids under plane-strain tension. Int. J. Solids. struct. 39, (2002) 983-1002.

[28] S.S. Campos, H.J. Kestenbach & E.V. Morales. On strengthening mechanisms in commercial Nb-Ti hot strip steels. Metall. Mater. Trans. A. 32, (2001) 1245-1248.

[29] L. Wu, T. Yao, Y. Wang, J. Zhang, F. Xiao & B. Liao. Understanding the mechanical properties of vanadium carbides: Nano-indentation measurement and first-principles calculations. J. Alloy. Compd. 548, (2013) 60-64.

[30] T. Gladman. Precipitation hardening in metals. Mater. Sci. Technol.15, (2013) 30-36.